Robotica (2016) volume 34, pp. 2241–2256. © Cambridge University Press 2015
doi:10.1017/S0263574714002860

Kinematic analysis of a novel 2(3-RUS) parallel manipulator

Róger E. Sánchez-Alonso†*, José-Joel González-Barbosa†, Eduardo Castillo-Castaneda† and Jaime Gallardo-Alvarado‡

†*Centro de Investigación en Ciencia Aplicada y Tecnología Avanzada, Instituto Politécnico Nacional. Cerro Blanco, No. 141, Colinas del Cimatario, Querétaro, QRO, México*
‡*Departamento de Ingeniería Mecánica, Instituto Tecnológico de Celaya. Av. Tecnológico y Av. García Cubas, No. 38010, Celaya, GTO, México*

(Accepted November 28, 2014. First published online: January 20, 2015)

SUMMARY
This paper introduces a novel 6-DOF parallel manipulator, which is composed of two 3-RUS parallel manipulators that share a common three-dimensional moving platform. Semi-analytical form solutions are easily obtained to solve the forward displacement analysis of the robot using the non-planar geometry of the moving platform, whereas the velocity, acceleration, and singularity analyses are performed using screw theory. A case study is included to show the application of the kinematic model, which is verified with the aid of a commercially available software. Simple kinematic analysis and reduced singular regions are the main benefits of the proposed parallel manipulator.

KEYWORDS: Parallel manipulators; Hexapods; Kinematic analysis; Semi-analytical form solution; Screw theory.

1. Introduction

After the contributions of Gough[1,2] and Stewart[3] to robotics engineering, many prototypes have been developed based on a parallel architecture. Some prototypes have had a great impact and have become a reality in the production lines in many industries around the world, e.g., the Delta robot created by Clavel[4,5] and the Tricept robot designed by Neuman.[6,7] However, other prototypes, most of which are hexapods, did not complete their transition from design laboratories to industry despite having huge potential.

One may think that hexapods have had slow progress in the industry because of their cost compared to other architectures with fewer degrees of freedom, but it is mostly because of their multiloop architecture, which makes the kinematic analysis challenging for the scientific community and developers of this type of manipulator.

Regarding the forward displacement analysis, this problem is considered one of the most attractive and challenging topics of modern kinematics because it is complicated to find a closed-form solution for this type of architecture. The problem is so difficult that some authors have shown that the model for a conventional hexapod yields 40 complex and real solutions.[8–12] Different algorithms have been developed to compute these solutions, e.g., elimination methods,[12–16] continuation methods,[11,17,18] Gröbner bases methods,[19,20] interval analyses[21,22] and more recently, the application of genetic algorithms[23–25] and neural networks.[26,27] However, the forward displacement analysis for hexapods remains an open problem for the scientific community. A practical method to overcome the problem is to use sensors in the passive joints,[28,29] which is also used to simplify the dynamics and control

* Corresponding author. E-mail: rogersan1984@hotmail.es

https://doi.org/10.1017/S0263574714002860 Published online by Cambridge University Press

of parallel mechanisms,[30] but this approach only avoids the complexity of the problem instead of solving it. Because of the difficulty of finding a closed-form solution, the topology of this type of manipulator has been modified, e.g., the incorporation of compound joints and the introduction of moving platforms with regular polyhedron shapes.[31–36] For compound joints, this widely used strategy is notably useful to facilitate the forward displacement model; however, its application is mainly theoretical because it is currently impossible to build such joints and incorporate them into the mechanism ensuring an appropriate mobility. On the other hand, the use of mobile platforms with regular polyhedron shapes has become an attainable and efficient strategy to simplify the forward displacement model in hexapods, as recently demonstrated in refs. [35, 36] for a manipulator that was inspired by the Gough–Stewart platform.

In addition to the forward displacement analysis, the existence of multiple singular configurations is another major drawback that prevents a greater presence of hexapods in the industry. Many works addressed the identification of these singular configurations[37–40] and singularity-free path planning;[41–43] however, according to the authors' knowledge, the development of a truly practical and achievable strategy to maximize the singularity-free workspace of these mechanisms has not been extensively studied.

Considering these two problems, in this work, a 2(3-RUS) parallel manipulator inspired by the Hexa robot[44] is introduced. The design strategy of the manipulator simplifies the forward displacement analysis to find a semi-analytical form solution, and allows one to avoid some typical singularities that are associated with this type of robot. The remainder of the contribution is organized as follows: In Section 2, the proposed parallel manipulator is outlined; in Section 3, the forward and inverse displacement analyses are presented; in Section 4, the velocity and acceleration analyses are performed using screw theory; in Section 5, the singular configurations are determined using the manipulator Jacobian matrices; finally, the discussion and a case study are presented in Section 6, where the obtained results with the proposed kinematic model are compared to a model that was generated using the simulation software ADAMS©.

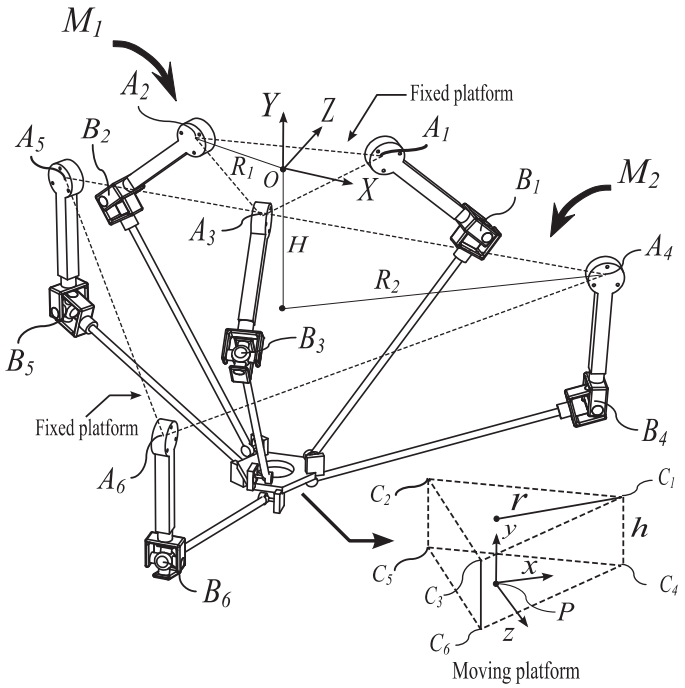
2. Description of the Proposed Parallel Manipulator

The proposed manipulator (patenting process: MX/a/2013/011009) consists of two 3-RUS parallel sub-manipulators, which share a common three-dimensional moving platform (Fig. 1a), where R, U, and S denote the revolute, universal and spherical joints, respectively, and the underline represents the active joint. Unless otherwise specified, hereafter, the subscripts $i = 1, 2, 3$ refer to elements of the sub-manipulator M_1, whereas the subscripts $i = 4, 5, 6$ refer to elements of the sub-manipulator M_2.

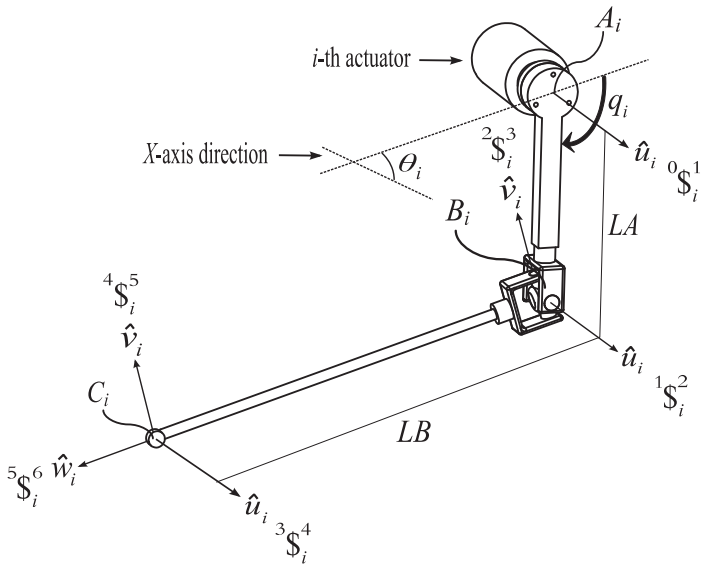
The fixed platform of the manipulator is represented by two parallel equilateral triangles $A_1A_2A_3$ and $A_4A_5A_6$, which are separated by a distance H. The fixed coordinate system is attached to the center O of the triangle $A_1A_2A_3$, its X- and Z-axes lie on the plane defined by this triangle, and the Y-axis points upward. The active revolute joints, whose nominal positions $A_i = (A_{Xi}, A_{Yi}, A_{Zi})$ are located by vectors $\boldsymbol{A}_i$, determine the vertices of the equilateral triangles $A_1A_2A_3$ and $A_4A_5A_6$, where R_1 and R_2 represent the circumradii of these triangles, and θ_i represents the orientation of the ith kinematic chain (Fig. 1b), which is measured from the X-axis direction to vector $\boldsymbol{A}_i$ for $i = 1, 2, 3$ and to the projection of vector $\boldsymbol{A}_i$ on the XZ plane for $i = 4, 5, 6$.

On the other hand, $B_i = (B_{Xi}, B_{Yi}, B_{Zi})$ denotes the nominal position, which is located by vectors $\boldsymbol{B}_i$, of the universal joint that connects the link of length LA to the link of length LB in the same kinematic chain. Similarly, $C_i = (C_{Xi}, C_{Yi}, C_{Zi})$ denotes the nominal position, which is located by vectors $\boldsymbol{C}_i$, of the spherical joint that connects the moving platform to the link of length LB. Points C_i form a triangular prism of height h defined by the equilateral triangles $C_1C_2C_3$ and $C_4C_5C_6$, where r represents the circumradius of these triangles. The rotation axes of the active revolute joints, which are denoted by $\hat{u}_i$, are tangential to the circumscribed circle of the triangles $A_1A_2A_3$ and $A_4A_5A_6$. Moreover, the rotation axes of the universal joints are $\hat{u}_i$ and $\hat{\boldsymbol{v}}_i$, where $\hat{\boldsymbol{v}}_i$ is orthogonal to $\hat{u}_i$ and to the direction $\hat{w}_i$ of the link of length LB. For the spherical joints, the rotation axes are $\hat{u}_i$, $\hat{\boldsymbol{v}}_i$ and $\hat{w}_i$. Finally, point $P = (P_X, P_Y, P_Z)$, which is located by vector $\boldsymbol{P}$, is the interest point in the moving platform (end effector) and is conveniently located at the center of the triangle $C_4C_5C_6$, which indicates that a moving coordinate system xyz is defined at this point.

https://doi.org/10.1017/S0263574714002860 Published online by Cambridge University Press



(a)



(b)

Fig. 1. Proposed manipulator. (a) General view; (b) the *i*th kinematic chain.

To verify the mechanism mobility, the Grübler–Kutzbach criterion may be applied, which is given by:

$$F = 6\,(n - p - 1) + \sum_{k=1}^{p} f_k \tag{1}$$

where F is the number of degrees of freedom, n is the number of links including the fixed platform, p is the number of joints, and f_k is the number of degrees of relative motion permitted by the kth

https://doi.org/10.1017/S0263574714002860 Published online by Cambridge University Press

joint. For the proposed manipulator, $n = 14$, $p = 6(\text{R}) + 6(\text{U}) + 6(\text{S}) = 18$ and $\sum f_k = 36$. Thus, the manipulator has 6-DOF.

3. Displacement Analysis

Because of the complexity of the forward displacement analysis for hexapods, a simple method is used in this paper to simplify the problem. This method is based on the idea that any point of a rigid body can be expressed as a linear combination of key points embedded in the same body.

The forward displacement analysis consists of finding the pose (position and orientation) of the moving platform with respect to the fixed platform for a given set of generalized coordinates q_i. To accomplish this task, the coordinates of $A_i = (A_{Xi}, A_{Yi}, A_{Zi})$ and $B_i = (B_{Xi}, B_{Yi}, B_{Zi})$ must be calculated as follows:

$$A_i = \begin{bmatrix} R\cos\theta_i \\ D \\ R\sin\theta_i \end{bmatrix} \tag{2}$$

$$B_i = \begin{bmatrix} A_{Xi} + LA\cos q_i\cos\theta_i \\ A_{Yi} + LA\sin q_i \\ A_{Zi} + LA\cos q_i\sin\theta_i \end{bmatrix} \tag{3}$$

where $R = R_1$ and $D = 0$ for $i = 1, 2, 3$, and $R = R_2$ and $D = -H$ for $i = 4, 5, 6$.

Moreover, considering that the moving platform is a triangular prism of height h, the coordinates of C_4, C_5, and C_6 may be written according to the coordinates of C_1, C_2, and C_3, respectively, as follows:

$$\boldsymbol{C}_{i+3} = \boldsymbol{C}_i + h\hat{g}, \quad \boldsymbol{i} = 1, 2, 3 \tag{4}$$

where $\hat{g}$ is a unit vector normal to the equilateral triangle $C_1C_2C_3$, which is computed using the usual cross product:

$$\hat{g} = \frac{2/3\sqrt{3}\,(\boldsymbol{C}_2 - \boldsymbol{C}_3) \times (\boldsymbol{C}_1 - \boldsymbol{C}_3)}{e^2} \tag{5}$$

where $e = 2r\cos(\pi/6)$ represents the side of the triangular prism that is defined by the moving platform.

Considering these conditions, the forward displacement analysis is reduced to find the coordinates of C_1, C_2, and C_3. Thus, we consider the following six closure equations:

$$(\boldsymbol{C}_i - \boldsymbol{B}_i) \bullet (\boldsymbol{C}_i - \boldsymbol{B}_i) = LB^2, \ i = 1, \ 2, \ldots 6 \tag{6}$$

where the bullet ($\bullet$) denotes the inner product of the conventional three-dimensional vectorial algebra.

Moreover, three compatibility closure equations may be written based on the geometry of the moving platform as:

$$\left(\boldsymbol{C}_i - \boldsymbol{C}_j\right) \bullet \left(\boldsymbol{C}_i - \boldsymbol{C}_j\right) = e^2, \quad (i, j) \in \left\{(1,2) \quad (2,3) \quad (1,3)\right\} \tag{7}$$

Expressions (6) and (7) form a system of nine quadratic equations and nine unknowns: C_{Xi}, C_{Yi}, and C_{Zi} for $i = 1, 2, 3$. Various methods have been developed to solve systems of nonlinear, multivariate polynomial equations. These methods have strengths and weaknesses, and the applicability of each method highly depends on the particular problem being addressed. The polynomial continuation method has proven to be a good alternative to solve this type of system because it is a numerical procedure that can find all solutions to a given problem,[45] unlike others that converge to a single solution, e.g., the Newton-Raphson method.

After the system is solved, C_{Xi}, C_{Yi}, and C_{Zi} for $i = 4, 5, 6$ may be computed using expression (4).

https://doi.org/10.1017/S0263574714002860 Published online by Cambridge University Press

To determine the pose of the moving platform, it is necessary to consider the moving coordinate system attached to the center of the equilateral triangle $C_4C_5C_6$ (Fig. 1a). This coordinate system has its x- and z-axes lying on the plane defined by the triangle, where the x-axis points to C_4. Thus, the position of the moving platform is defined by vector $\boldsymbol{P}$ as follows:

$$\boldsymbol{P} = \frac{1}{3}\sum_{i=4}^{6} \boldsymbol{C}_i \tag{8}$$

whereas, the orientation is defined by a rotation matrix $\boldsymbol{R_m}$ using the method introduced in ref. [46]. The rotation matrix $\boldsymbol{R_m}$ is defined as:

$$\boldsymbol{R_m} = \begin{bmatrix} \hat{u}_x & \hat{u}_y & \hat{u}_z \end{bmatrix} \tag{9}$$

where $\hat{u}_x, \hat{u}_y, \hat{u}_z$ are unit vectors along the axes of the moving coordinate system and may be computed as follows:

$$\hat{u}_x = \frac{\boldsymbol{C}_4 - \boldsymbol{P}}{\|\boldsymbol{C_4} - \boldsymbol{P}\|} \tag{10}$$

$$\hat{u}_z = \frac{\boldsymbol{C_6} - \boldsymbol{C_5}}{\|\boldsymbol{C_6} - \boldsymbol{C_5}\|} \tag{11}$$

$$\hat{u}_y = \hat{u}_z \times \hat{u}_x \tag{12}$$

Finally, the pose of the moving platform is interpreted as the well-known 4 × 4 homogeneous transformation matrix $\boldsymbol{T}$, which is defined as:

$$\boldsymbol{T} = \begin{bmatrix} \boldsymbol{R_m} & \boldsymbol{P} \\ \boldsymbol{0} & \boldsymbol{1} \end{bmatrix} \tag{13}$$

On the other hand, the inverse displacement analysis consists of finding the generalized coordinates q_i for a given pose of the moving platform. Hence, the coordinates of C_i may be computed based on the following relationship:

$$\begin{bmatrix} C_i \\ 1 \end{bmatrix} = \boldsymbol{T} \begin{bmatrix} C_i^* \\ 1 \end{bmatrix} \tag{14}$$

where C_i^* is known and represents the coordinates of C_i but is expressed in the moving coordinate system.

The substitution of (3) and (14) into Eq. (6) yields the following expression for q_i:

$$\tan\frac{q_i}{2} = \frac{2C_{Yi} - 2D \pm \sqrt{4\left(D - C_{Yi}\right)^2 + 4R^2 - S_i^2 - Q_i\left(4R + \frac{2S_iR}{LA}\right) + Q_i^2\left(1 - \frac{R^2}{LA^2}\right)}}{-2R - S_i - Q_i\left(\frac{R}{LA} - 1\right)} \tag{15}$$

where:

$$S_i = \frac{1}{LA}\left(LB^2 - LA^2 - R^2 - D^2 + 2DC_{Yi} - C_{Xi}^2 - C_{Yi}^2 - C_{Zi}^2\right) \tag{16}$$

$$Q_i = 2C_{Xi}\cos\theta_i + 2C_{Zi}\sin\theta_i \tag{17}$$

where $R = R_1$ and $D = 0$ for $i = 1, 2, 3$, and $R = R_2$ and $D = -H$ for $i = 4, 5, 6$.

4. Velocity and Acceleration Analysis

The velocity and acceleration analyses are addressed using screw theory. For a detailed explanation of the method of infinitesimal kinematics that we used here, please consult refs. [47–49].

https://doi.org/10.1017/S0263574714002860 Published online by Cambridge University Press

The screws that are associated with each joint of the *i*th kinematic chain (Fig. 1b) are: ${}^{0}\$_i^1$, which is associated with the active revolute joint; ${}^{1}\$_i^2$ and ${}^{2}\$_i^3$, which intersect point B_i and address the universal joint that connects the link of length *LA* to the link of length *LB*; and ${}^{3}\$_i^4$, ${}^{4}\$_i^5$, and ${}^{5}\$_i^6$, which intersect point C_i and address the spherical joint that connects the moving platform to the link of length *LB*.

A screw is defined in Plücker coordinates as: ${}^{j-1}\$_i^j = [\,{}^{j-1}S_i^j \;\; {}^{j-1}SO_i^j\,]^T$ for $j = 1, 2, \ldots 6$, where ${}^{j-1}S_i^j$, which is the primal part, is a unit vector along the rotation axis of the joint associated with the screw ${}^{j-1}\$_i^j$, whereas ${}^{j-1}SO_i^j$, which is the dual part, is the moment produced by ${}^{j-1}S_i^j$ about the reference pole *O*. Considering these definitions, the screws of the *i*th kinematic chain are: ${}^{0}\$_i^1 = [\,\hat{u}_i \;\; A_i \times \hat{u}_i\,]^T$, ${}^{1}\$_i^2 = [\,\hat{u}_i \;\; B_i \times \hat{u}_i\,]^T$, ${}^{2}\$_i^3 = [\,\hat{v}_i \;\; B_i \times \hat{v}_i\,]^T$, ${}^{3}\$_i^4 = [\,\hat{u}_i \;\; C_i \times \hat{u}_i\,]^T$, ${}^{4}\$_i^5 = [\,\hat{v}_i \;\; C_i \times \hat{v}_i\,]^T$, ${}^{5}\$_i^6 = [\,\hat{w}_i \;\; C_i \times \hat{w}_i\,]^T$. For more information about the screw definition, please consult ref. [50].

The velocity state $\boldsymbol{V}$ of the moving platform may be expressed in screw form as:

$$\boldsymbol{V} = \begin{bmatrix} \boldsymbol{\omega} \\ \boldsymbol{v} \end{bmatrix} = {}_0\boldsymbol{\omega}_1^i \, {}^{0}\$_i^1 + {}_1\boldsymbol{\omega}_2^i \, {}^{1}\$_i^2 + {}_2\boldsymbol{\omega}_3^i \, {}^{2}\$_i^3 + {}_3\boldsymbol{\omega}_4^i \, {}^{3}\$_i^4 + {}_4\boldsymbol{\omega}_5^i \, {}^{4}\$_i^5 + {}_5\boldsymbol{\omega}_6^i \, {}^{5}\$_i^6 \tag{18}$$

where $\boldsymbol{\omega}$ and $\boldsymbol{v}$ are the angular and linear velocity vectors of the moving platform, respectively, with respect to the fixed platform, and ${}_{j-1}\omega_j^i$ is the joint velocity rate associated with the *j*th screw of the *i*th kinematic chain, and ${}_0\omega_1^i = \dot{q}_i$ is the *i*th generalized velocity of the robot.

Expression (18) may be rewritten in compact form as follows:

$$\boldsymbol{V} = \boldsymbol{J_i}\boldsymbol{\Omega}_{\mathrm{i}} \tag{19}$$

where $\boldsymbol{J_i} = [\,{}^{0}\$_i^1 \;\; {}^{1}\$_i^2 \;\; {}^{2}\$_i^3 \;\; {}^{3}\$_i^4 \;\; {}^{4}\$_i^5 \;\; {}^{5}\$_i^6\,]$ is the screw-coordinate Jacobian matrix of the *i*th kinematic chain, and $\boldsymbol{\Omega_i} = [\,{}_0\omega_1^i \;\; {}_1\omega_2^i \;\; {}_2\omega_3^i \;\; {}_3\omega_4^i \;\; {}_4\omega_5^i \;\; {}_5\omega_6^i\,]^T$ is the vector of joint-velocity rates of the same chain.

To obtain the input–output equation of velocity of the robot, it is necessary to consider the screw ${}^{5}\$_i^6$, which is reciprocal to all screws in the same kinematic chain, except the screw that is associated with the actuated revolute joint ${}^{0}\$_i^1$. Hence, the application of the Klein form $\{*\,;\,*\}$, which is a bilinear symmetric form of Lie algebra, of the screw ${}^{5}\$_i^6$ to both sides of expression (18) with the reduction of terms yields the following:

$$\left\{\boldsymbol{V}; {}^{5}\$_i^6\right\} = \dot{q}_i \left\{{}^{0}\$_i^1; {}^{5}\$_i^6\right\} \tag{20}$$

For a quick review of the screw theory basic operations, including the Klein form, please consult ref. [51].

If we present expression (20) in a matrix–vector form, the input–output equation of velocity of the parallel manipulator results in:

$$\boldsymbol{J}_{\boldsymbol{x}}^T \Delta \boldsymbol{V} = \boldsymbol{J_q}\dot{\boldsymbol{q}} \tag{21}$$

where:

$$\boldsymbol{J}_x = \left[\, {}^{5}\$_1^6 \quad {}^{5}\$_2^6 \quad {}^{5}\$_3^6 \quad {}^{5}\$_4^6 \quad {}^{5}\$_5^6 \quad {}^{5}\$_6^6 \,\right] \tag{22}$$

is the active screw-coordinate Jacobian matrix of the manipulator, whereas $\boldsymbol{J_q}$ is a diagonal matrix given by:

$$\boldsymbol{J_q} = \mathrm{diag}\left[\, \left\{{}^{0}\$_1^1; {}^{5}\$_1^6\right\} \quad \left\{{}^{0}\$_2^1; {}^{5}\$_2^6\right\} \quad \left\{{}^{0}\$_3^1; {}^{5}\$_3^6\right\} \quad \left\{{}^{0}\$_4^1; {}^{5}\$_4^6\right\} \quad \left\{{}^{0}\$_5^1; {}^{5}\$_5^6\right\} \quad \left\{{}^{0}\$_6^1; {}^{5}\$_6^6\right\} \,\right] \tag{23}$$

and:

$$\Delta = \begin{bmatrix} \boldsymbol{0} & \boldsymbol{I} \\ \boldsymbol{I} & \boldsymbol{0} \end{bmatrix} \tag{24}$$

https://doi.org/10.1017/S0263574714002860 Published online by Cambridge University Press

is an operator of polarity in terms of the 3×3 identity matrix $\boldsymbol{I}$ and 3×3 zero matrix $\boldsymbol{0}$. Furthermore, $\dot{\boldsymbol{q}}$ is the first-order driver matrix of the robot, which is given by:

$$\dot{\boldsymbol{q}} = \begin{bmatrix} \dot{q}_1 & \dot{q}_2 & \dot{q}_3 & \dot{q}_4 & \dot{q}_5 & \dot{q}_6 \end{bmatrix}^T \tag{25}$$

The forward velocity analysis consists of finding the velocity state $\boldsymbol{V}$ of the moving platform for a given set of generalized velocities $\dot{q}_i$, which may be easily computed using expression (21).

After the velocity state is computed, the velocity of point P may be obtained using classical kinematics as follows:

$$\boldsymbol{v_P} = \boldsymbol{v} + \boldsymbol{\omega} \times \boldsymbol{P} \tag{26}$$

On the other hand, the inverse velocity analysis consists of finding the joint-velocity rates ${}_{j-1}\boldsymbol{\omega}^i_j$ for a given velocity state, which may be computed using expression (19).

Following the kinematic analysis, in 1947, Brand introduced the concept of reduced acceleration state of a rigid body, which was defined as:

$$\boldsymbol{A} = \begin{bmatrix} \dot{\boldsymbol{\omega}} \\ \boldsymbol{a} - \boldsymbol{\omega} \times \boldsymbol{v} \end{bmatrix} \tag{27}$$

where $\dot{\boldsymbol{\omega}}$ and $\boldsymbol{a}$ are the angular and linear acceleration vectors of the moving platform with respect to the fixed platform, respectively.

The acceleration state may be expressed in screw form as:

$$\boldsymbol{A} = {}_0\dot{\omega}^i_1 {}^0\$^1_i + {}_1\dot{\omega}^i_2 {}^1\$^2_i + {}_2\dot{\omega}^i_3 {}^2\$^3_i + {}_3\dot{\omega}^i_4 {}^3\$^4_i + {}_4\dot{\omega}^i_5 {}^4\$^5_i + {}_5\dot{\omega}^i_6 {}^5\$^6_i + \mathcal{L}_i \tag{28}$$

where ${}_{j-1}\dot{\omega}^i_j$ is the join-acceleration rate associated with the jth screw of the ith kinematic chain, and ${}_0\dot{\omega}^i_1 = \ddot{q}_i$ is the ith active angular acceleration of the robot. Furthermore, $\mathcal{L}_i$ is the ith Lie screw of acceleration, which is computed as:

$$\begin{aligned} \mathcal{L}_i = & \left[{}_0\omega^i_1 {}^0\$^1_i \;\; {}_1\omega^i_2 {}^1\$^2_i + {}_2\omega^i_3 {}^2\$^3_i + {}_3\omega^i_4 {}^3\$^4_i + {}_4\omega^i_5 {}^4\$^5_i + {}_5\omega^i_6 {}^5\$^6_i \right] \\ & + \left[{}_1\omega^i_2 {}^1\$^2_i \;\; {}_2\omega^i_3 {}^2\$^3_i + {}_3\omega^i_4 {}^3\$^4_i + {}_4\omega^i_5 {}^4\$^5_i + {}_5\omega^i_6 {}^5\$^6_i \right] \\ & + \left[{}_2\omega^i_3 {}^2\$^3_i \;\; {}_3\omega^i_4 {}^3\$^4_i + {}_4\omega^i_5 {}^4\$^5_i + {}_5\omega^i_6 {}^5\$^6_i \right] \\ & + \left[{}_3\omega^i_4 {}^3\$^4_i \;\; {}_4\omega^i_5 {}^4\$^5_i + {}_5\omega^i_6 {}^5\$^6_i \right] + \left[{}_4\omega^i_5 {}^4\$^5_i \;\; {}_5\omega^i_6 {}^5\$^6_i \right] \end{aligned} \tag{29}$$

where the brackets $[* \;\; *]$ denote the Lie product of Lie algebra. Naturally, the computation of the Lie screw of acceleration requires the solution of the velocity analysis of the robot. For a quick review of the screw theory basic operations, including the Lie product, please consult ref. [51].

Expression (28) may be rewritten in compact form as follows:

$$\boldsymbol{A} = \boldsymbol{J_i}\dot{\boldsymbol{\Omega}}_{\mathbf{i}} + \mathcal{L}_i \tag{30}$$

where $\dot{\boldsymbol{\Omega}}_i = [\, {}_0\dot{\omega}^i_1 \;\; {}_1\dot{\omega}^i_2 \;\; {}_2\dot{\omega}^i_3 \;\; {}_3\dot{\omega}^i_4 \;\; {}_4\dot{\omega}^i_5 \;\; {}_5\dot{\omega}^i_6 \,]^T$ is the vector of join-acceleration rates associated with the screws of the ith kinematic chain.

Similar to the velocity analysis, the systematic application of the Klein form $\{*\,;\,*\}$ of the screw ${}^5\$^6_i$ to both sides of expression (28) with the reduction of terms yields the following:

$$\left\{A\,;{}^5\$^6_i\right\} = \ddot{q}_i \left\{{}^0\$^1_i;{}^5\$^6_i\right\} + \left\{\mathcal{L}_i;{}^5\$^6_i\right\} \tag{31}$$

If expression (31) is presented in a matrix–vector form, the input–output equation of acceleration of the parallel manipulator results in:

$$\boldsymbol{J}^T_x \Delta \boldsymbol{A} = \boldsymbol{J_q}\ddot{\boldsymbol{q}} + \boldsymbol{C} \tag{32}$$

https://doi.org/10.1017/S0263574714002860 Published online by Cambridge University Press

where:

$$\ddot{\boldsymbol{q}} = \begin{bmatrix} \ddot{q}_1 & \ddot{q}_2 & \ddot{q}_3 & \ddot{q}_4 & \ddot{q}_5 & \ddot{q}_6 \end{bmatrix}^T \tag{33}$$

is the second-order driver matrix of the robot, and $\boldsymbol{C}$ is the complementary matrix of acceleration, which is given by:

$$C = \begin{bmatrix} \{\mathcal{L}_1; {}^5\$_1^6\} \\ \{\mathcal{L}_2; {}^5\$_2^6\} \\ \{\mathcal{L}_3; {}^5\$_3^6\} \\ \{\mathcal{L}_4; {}^5\$_4^6\} \\ \{\mathcal{L}_5; {}^5\$_5^6\} \\ \{\mathcal{L}_6; {}^5\$_6^6\} \end{bmatrix} \tag{34}$$

The forward acceleration analysis consists of finding the acceleration state $\boldsymbol{A}$ of the moving platform for a given set of active angular accelerations $\ddot{q}_i$, which may be easily computed using expression (32).

After the acceleration state is computed, the acceleration of point P may be obtained using classical kinematics as:

$$\boldsymbol{a_P} = \boldsymbol{a} + \dot{\boldsymbol{\omega}} \times \boldsymbol{P} + \boldsymbol{\omega} \times (\boldsymbol{\omega} \times \boldsymbol{P}) \tag{35}$$

where:

$$\boldsymbol{a} = \text{Dual}\,(\boldsymbol{A}) + \boldsymbol{\omega} \times \boldsymbol{v} \tag{36}$$

and Dual($\boldsymbol{A}$) refers to the dual part of the acceleration state $\boldsymbol{A}$.

On the other hand, the inverse acceleration analysis consists of finding the join-acceleration rates ${}_{j-1}\dot{\omega}_j^i$ for a given acceleration state, which may be computed using expression (30).

5. Singularity Analysis

For parallel robots, singularities are configurations where the moving platform gains or loses degrees of freedom. To identify these configurations, relationship (21) is fundamental. This expression relates the generalized velocities of the robot to the velocity state of the moving platform using two Jacobian matrices.

With classical approaches, these Jacobian matrices are functions of the sums and products of sines and cosines of the angles formed by active and passive joints,[50] where finding the singular configurations is somewhat complicated. However, using screw theory, this task becomes notably easy.

The singular configurations may be classified into three types, each of which has a specific physical interpretation.[52]

Singularity type 1. This singularity occurs when $\det(\boldsymbol{J}_q) = 0$, which arises when any diagonal element of $\boldsymbol{J}_q$ vanishes. Physically, this condition implies that at least one kinematic chain is in a full stretched-out or folded-back configuration, which makes ${}^0\$_i^1$ and ${}^5\$_i^6$ reciprocal and $\{{}^0\$_i^1; {}^5\$_i^6\} = 0$. An example of this type of singularity is shown in Fig. 2a, where the kinematic chains of the sub-manipulator M_1 are in a full stretched-out configuration.

Singularity type 2. This singularity occurs when $\det(\boldsymbol{J}_x) = 0$, which arises when the reciprocal screws ${}^5\$_i^6$ are linearly dependent. Because of the arrangement of the spherical joints in two parallel planes, the probability of occurrence of this condition is notably low. However, the manipulator can be in a singular configuration if the screws $[{}^5\$_1^6\ {}^5\$_2^6\ {}^5\$_3^6]$or $[{}^5\$_4^6\ {}^5\$_5^6\ {}^5\$_6^6]$ are linearly dependent; the former is because the robot may be seen as two 3-RUS parallel sub-manipulators (Fig. 1a). This situation may occur, e.g., when for any sub-manipulator, the links of length LB are located in the same plane and their reciprocal screws converge to a common point or are parallel, as happens in a plane mechanism.[53] An example of this situation is shown in Fig. 2b. To prevent this situation, the following relation must be satisfied: $LB + r > LA + R$, where $R = R_1$ for the sub-manipulator M_1 and $R = R_2$ for the sub-manipulator M_2. If this condition is only satisfied for one sub-manipulator,

https://doi.org/10.1017/S0263574714002860 Published online by Cambridge University Press

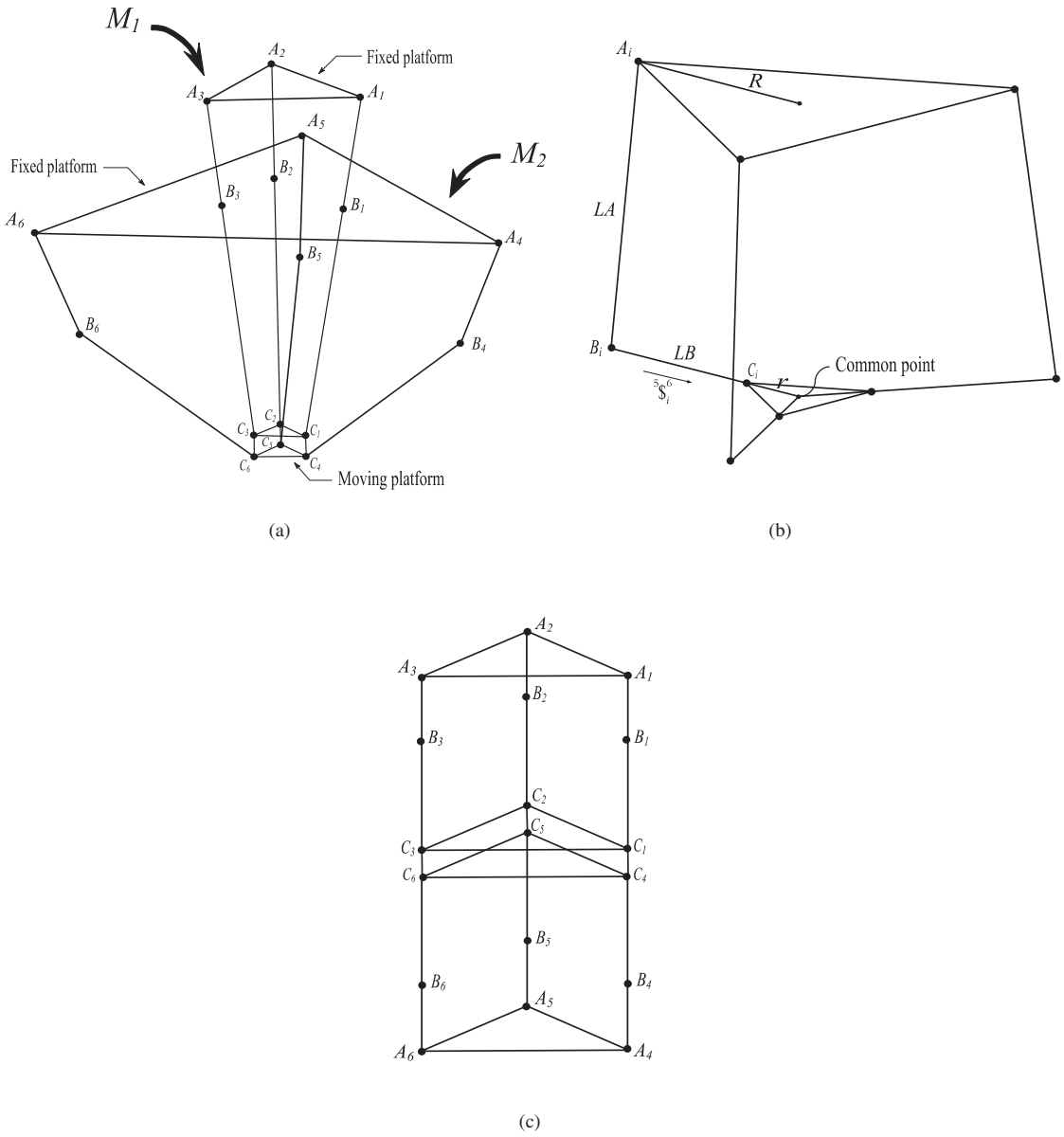


Fig. 2. Some singular poses of the parallel manipulator. (a) Singularity type 1; (b) Singularity type 2; (b) Singularity type 3.

this sub-manipulator can pull or push the other to avoid a singularity in the robot or release it if it already exists.

A special case of this type of singularity occurs when a row or column of $\boldsymbol{J_x}$ vanishes, e.g., when the equilateral triangles $A_1A_2A_3$ and $A_4A_5A_6$ (fixed platform) and $C_1C_2C_3$ and $C_4C_5C_6$ (moving platform) coincide, i.e., they are concentric and have identical orientations. Naturally, this condition can only arise along the negative Y direction. If this condition is satisfied, the second element in the dual part of the screws ${}^5\$_i^6$ of $\boldsymbol{J_x}$ is zero, which makes $\det(\boldsymbol{J_x}) = 0$ because the direction of ${}^5\$_i^6$ (primal part) and the location vector $\boldsymbol{C_i}$ of each spherical joint form an orthogonal plane to the XZ plane, which makes the dual part of ${}^5\$_i^6$ a vector of the plane XZ without the Y component. This singular configuration may be easily avoided if the orientations of $A_1A_2A_3$ and $A_4A_5A_6$ are properly selected to prevent all triangles from coinciding, considering the following condition: $\theta_i \neq \theta_{i+3}$, as shown in the case study in Section 6. This condition can generate collisions among the kinematic chains; thus, selecting the orientations of $A_1A_2A_3$ and $A_4A_5A_6$ is an interesting task to discuss in a future work related to the dimensional synthesis of the mechanism. According to the authors' knowledge, this singularity has not been reported in the literature, and to identify it is almost intuitive using screw theory.

https://doi.org/10.1017/S0263574714002860 Published online by Cambridge University Press

Singularity type 3. This singularity occurs when $\det(\boldsymbol{J_q}) = \det(\boldsymbol{J_x}) = 0$, which can arise if, e.g., any kinematic chain of a sub-manipulator is in a full stretched-out or folded-back configuration, whereas in the other sub-manipulator, the reciprocal screws are coplanar and converge to a common point. Another possible situation that involves this type of singularity is if the fixed and the moving platforms are identical in size, i.e., $A_1A_2A_3 = A_4A_5A_6 = C_1C_2C_3 = C_4C_5C_6$, and the kinematic chains are all vertical (naturally parallel), which occurs only if the moving platform is located between triangles $A_1A_2A_3$ and $A_4A_5A_6$, which is a meaningless configuration for the robot (Fig. 2c).

6. Discussion and Case Study

After studying the geometry and developing the kinematic model of the robot, we observe two significant characteristics in the proposed manipulator: (i) the relative geometrical independence between the sub-manipulators M_1 and M_2 and (ii) the triangular prism shape of the moving platform. The two sub-manipulators have relative geometrical independence because the equilateral triangles $A_1A_2A_3$ and $A_4A_5A_6$ are arranged in two parallel planes, which are separated by a distance H (Fig. 1a). Because this characteristic makes the geometry of the sub-manipulators practically independent of each other, the dimensions of each sub-manipulator can be properly selected to reduce or prevent collisions among the links, which are caused by the joint arrangement in the moving platform because of its triangular prism shape. Thus, these characteristics are complementary.

These characteristics belong to a design strategy that provides many kinematic advantages. From the theoretical analysis viewpoint, a semi-analytical form solution is easily obtained to solve the forward displacement analysis of the robot using the non-planar geometry of the moving platform, which represents a notably difficult task for a conventional hexapod. For practical application, the proposed robot can perform the same tasks as a conventional hexapod, but its applications increase because of the reduced presence of singular configurations compared to other hexapods, particularly singularity type 2.

The strategy of using moving platforms for hexapods with polyhedron shapes has been applied[31–36]; however, for the architecture in refs. [31–34], the kinematic chains begin from the same plane, which obviously causes a limited orientation capability in the robot. The architecture introduced in refs. [35, 36] has few practical applications because the available space for machining, assembly and any other task is reduced or almost null. In addition, the aforementioned structures are designed for only machining tasks; thus, they have linear actuators.

The proposed mechanism consists of six notably simple and lightweight kinematic chains, which are driven by rotational actuators. This actuation scheme makes the robot faster than those equipped with linear actuators, which represents an interesting alternative for industry, specifically for packaging tasks and high-speed/high-precision assembly or light machining. In fact, there are many applications for this mechanism: it can be used as a medical device in the rehabilitation of patients with upper extremity problems (shoulder, elbow, and wrist) or high-precision 3D printers; the application will depend on how the user wants to take advantage of the robot kinematics.

Regarding the proposed kinematic model, a case study is presented below to show its application. This case study consists of two parts: in the first part, the inverse displacement analysis was applied for a defined path, and the results were used in the second part, where the forward displacement model and the velocity and acceleration analyses were addressed. To develop this numerical example, the geometrical parameters of the robot are listed in Table I. Calculations were performed on a personal computer: Intel Xeon 2 CPU 3.20 GHz, 4.00 GB RAM, with Microsoft Windows 7 Pro. 64-bits Operating System.

First part. The inverse displacement analysis was applied for a path that was defined by the following 4×4 homogeneous transformation matrix:

$$\boldsymbol{T}(t) = \begin{bmatrix} 0.64 & -0.03 & 0.76 & -0.96t\cos t + 1.14t\sin t - 36.79 \\ 0.40\cos\psi + 0.64\sin\psi & 0.86\cos\psi - 0.49\sin\psi & -0.29\cos\psi - 0.57\sin\psi & -0.60t\,rmcos\,t - 0.44t\sin t - 461.65 \\ -0.64\cos\psi + 0.40\sin\psi & 0.49\cos\psi + 0.86\sin\psi & 0.57\cos\psi - 0.29\sin\psi & 0.97t\,rmcos\,t + 0.86t\sin t - 4.74 \\ 0 & 0 & 0 & 1 \end{bmatrix}$$

where $\psi = 0.1745\sin t$ rad., and the time interval of $0 \leq t \leq 8\pi$ s was divided into 500 steps.

https://doi.org/10.1017/S0263574714002860 Published online by Cambridge University Press

Table I. Geometrical parameters of the robot.

Parameter	Value
R_1	150 mm
R_2	450 mm
H	200 mm
LA	200 mm
LB	400 mm
h	34 mm
r	50 mm
θ_1	-35°
θ_2	-155°
θ_3	-275°
θ_4	-25°
θ_5	-145°
θ_6	-265°

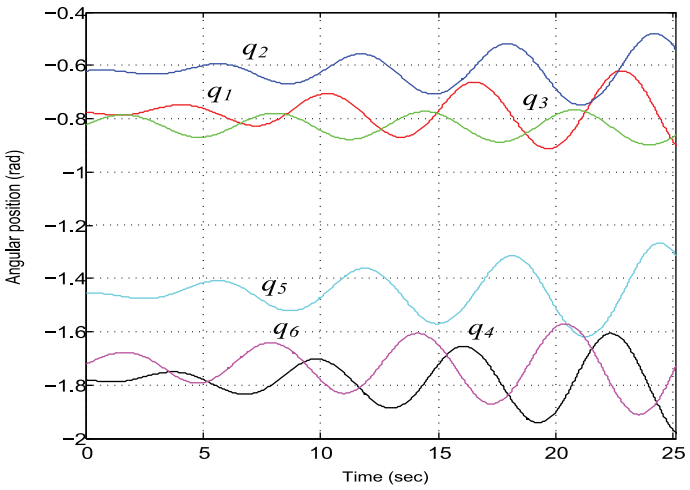


Fig. 3. Generalized coordinates.

Note that $\boldsymbol{T}(t)$ represents a motion where the position and orientation of the moving platform are functions of time. Specifically, the moving platform simultaneously rotates when the interest point P (end effector) describes a spiral path that is traced on an inclined plane starting at point $P(0) = (-36.79, -461.65, -4.74)$.

The solution to this part is to find the generalized coordinates $q_i(t)$. The application of expression (15) for the proposed inverse displacement model yields the periodical functions in Fig. 3. The computation time is approximately 0.1804 s.

Second part. The purpose is to find the position, velocity and acceleration of the interest point P (end effector) by considering the temporal behavior of the generalized coordinates, which were obtained in the first part. The results of the proposed kinematic model were compared to a model generated using the simulation software ADAMS©.

For the forward displacement analysis, this process is developed in two stages. The first stage involves solving the proposed model at time $t = 0$, i.e., when the generalized coordinates are approximately $q_1 = -0.7755$, $q_2 = -0.6214$, $q_3 = -0.8242$, $q_4 = -1.7798$, $q_5 = -1.4532$, and $q_6 = -1.7233$. To achieve this goal, the system of equations, which was derived from expressions (6) and (7), is solved using a publicly available computer package based on numerical homotopy continuation methods,[54] which results in 40 solutions for C_1, C_2, and C_3, four of which are real. The real solutions are listed in Table II, and a graphical representation of these solutions is shown in Fig. 4. The computation time is approximately 1,413.2670 s.

https://doi.org/10.1017/S0263574714002860 Published online by Cambridge University Press

Table II. Real solutions of the forward displacement analysis ($t = 0$).

Sol.	C_1	C_2	C_3
1	(−5.3,657, −422.4,890, −26.2,495)	(−86.8,122, −439.8,238, −2.4,596)	(−20.7,645, −465.4,835, 47.3,326)
2	(7.5,073, −426.8,699, −13.8959)	(−60.5,726, −441.8,911, −65.2717)	(−72.2,179, −430.2,709, 19.7538)
3	(−13.3,077, −402.5,441, −3.6614)	(−89.8,259, −443.0335, −6.0213)	(−29.8,183, −467.1,774, 51.5647)
4	(−16.1,519, −399.4,689, −3.1,841)	(−89.4,443, −444.8,543, −11.4,535)	(−32.3,055, −465.7,321, 50.1,846)

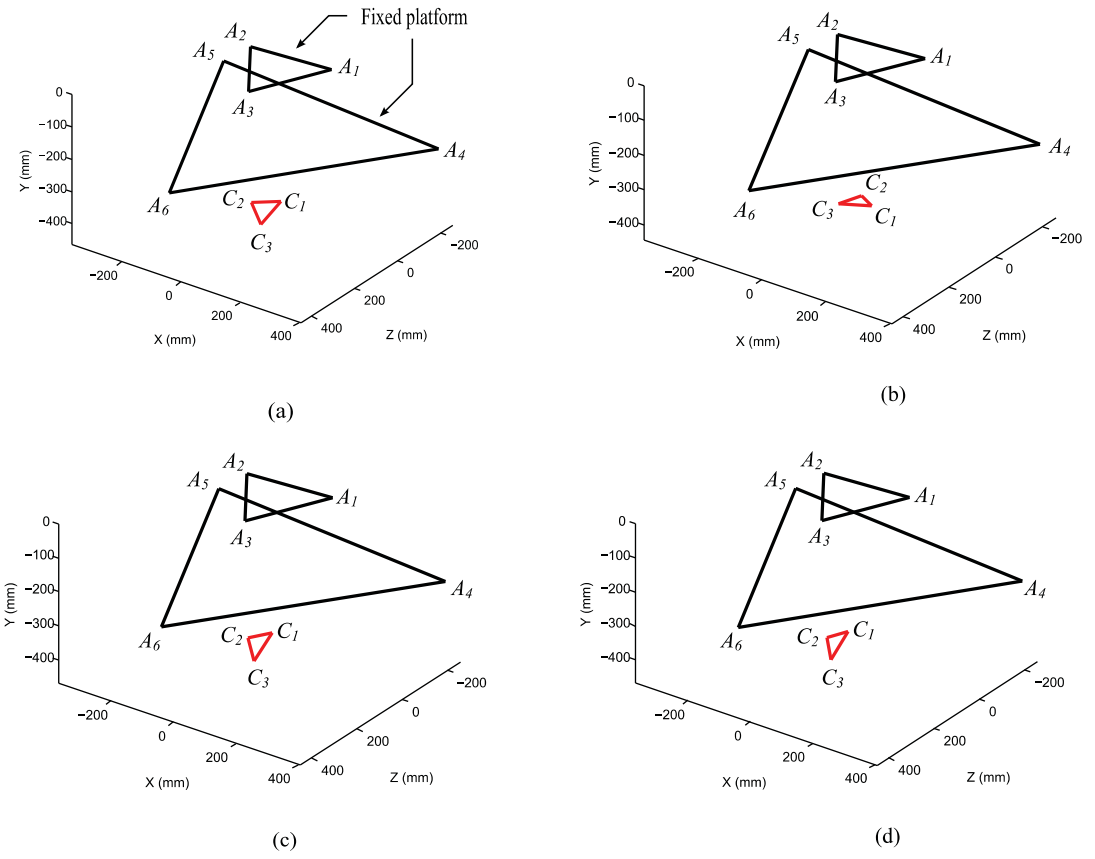


Fig. 4. Real solutions of the forward displacement analysis ($t = 0$). (a) Sol. 1; (b) Sol. 2; (c) Sol. 3; (d) Sol. 4.

Remember that the coordinates of C_4, C_5, and C_6 are obtained from the coordinates of C_1, C_2, and C_3, respectively, using expression (4), with which the coordinates of point P may be computed using expression (8).

In the second stage, to approach the forward displacement analysis for the entire path, the Multivariate Newton-Raphson method was applied by considering solution 1 of Table II as the reference configuration of the manipulator (initial value). Figure 5 presents the results of the proposed model compared to those of the software ADAMS©, where it is noticeable that the numerical results are significantly consistent with the simulation. In fact, there is a perfect consistency between the two models up to the third decimal, i.e., the deviations are on the order of ten thousandths of a millimeter. The computation time is approximately 1.9844 s.

After the forward displacement analysis is solved, the velocity and acceleration models based on screw theory may be performed. It is important to mention that the generalized velocities and active

https://doi.org/10.1017/S0263574714002860 Published online by Cambridge University Press

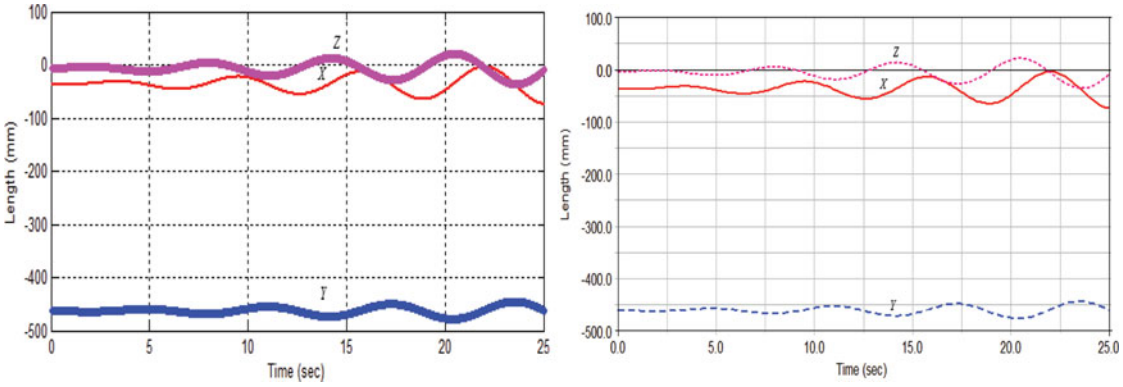


Fig. 5. Position of point P for the entire path. Left: results of the proposed forward displacement model; right: results using ADAMS©.

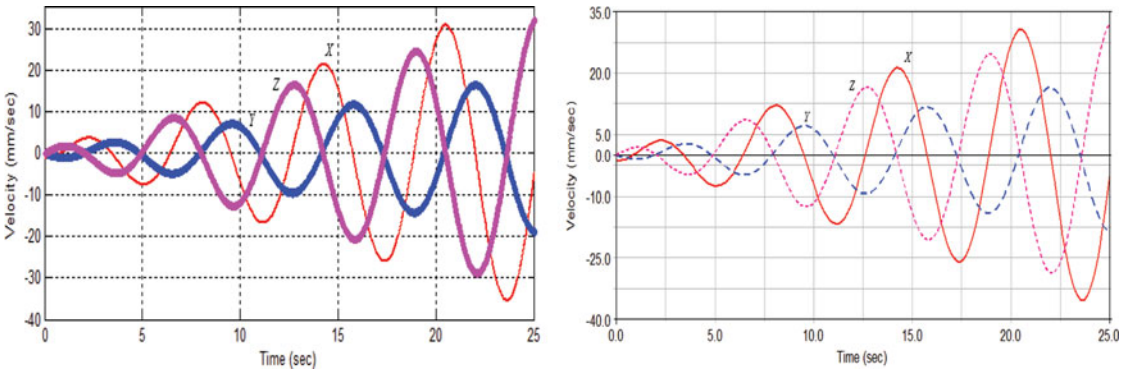


Fig. 6. Velocity of point P for the entire path. Left: results of the proposed forward velocity model; right: results using ADAMS©.

angular accelerations are obtained using the first- and second-order numerical differentiation of the generalized coordinates, respectively. The velocity results of point P are shown in Fig. 6, where an excellent consistency with the simulation in ADAMS© is observed. Considering the ADAMS© results as a reference, the relative error of the proposed velocity model for the trajectory under study is shown in Fig. 7. Note that the error has a cyclical behavior for the X, Y, and Z components of the velocity, and the largest deviation is on the order of $\pm 0.4\%$.

The acceleration results of point P are presented in Fig. 8. Similarly, to validate the results, a simulation was performed using the software ADAMS©. The numerical results are significantly consistent with the simulation; the relative error has a cyclical behavior for the X, Y, and Z components of the acceleration, and the largest deviation is on the order of $\pm 0.5\%$ (Fig. 9).

The computation time to implement the proposed velocity and acceleration models is approximately 9.9344 s.

7. Conclusions

Kinematic analysis for hexapods is a complicated open problem in the scientific community. Regarding the forward displacement analysis, it is complicated to find a closed-form solution because of the multiloop architecture. The problem is extremely complicated regardless of the method to solve it, such as elimination methods, continuation methods, Gröbner bases, etc. On the other hand, the existence of multiple singular configurations is also a serious problem in such mechanisms.

Considering the above, in this work, a hexapod inspired by the Hexa robot was introduced. The proposed manipulator consists of two 3-RUS parallel sub-manipulators, where the fixed platform is represented by two triangles, which were arranged in parallel planes. Both sub-manipulators are joined in the moving platform, which has a triangular prism shape. The characteristics of the proposed manipulator, specifically the relative geometrical independence between the sub-manipulators and

https://doi.org/10.1017/S0263574714002860 Published online by Cambridge University Press

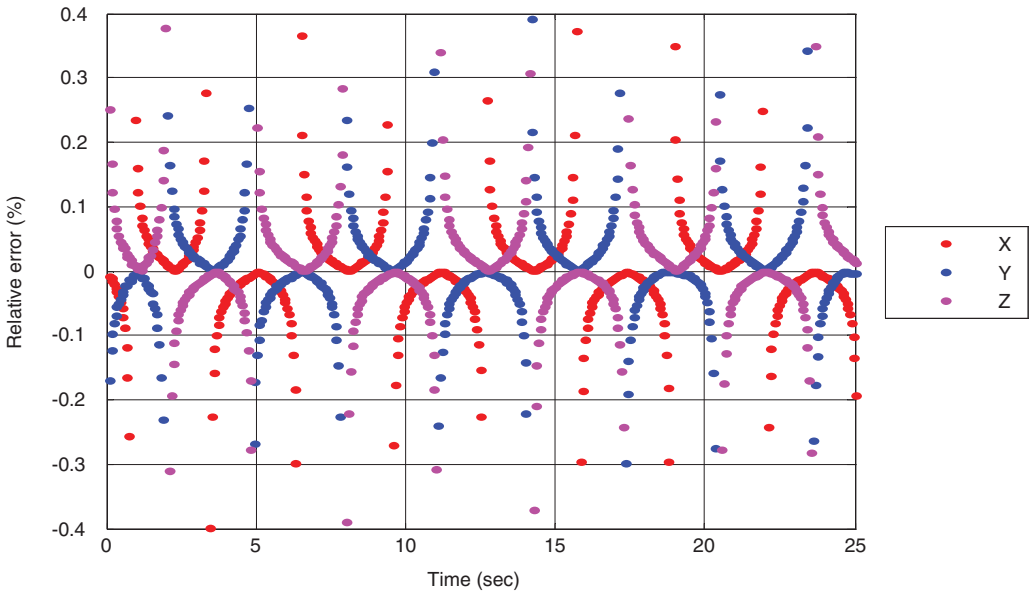


Fig. 7. Relative error of the velocity model based on screw theory.

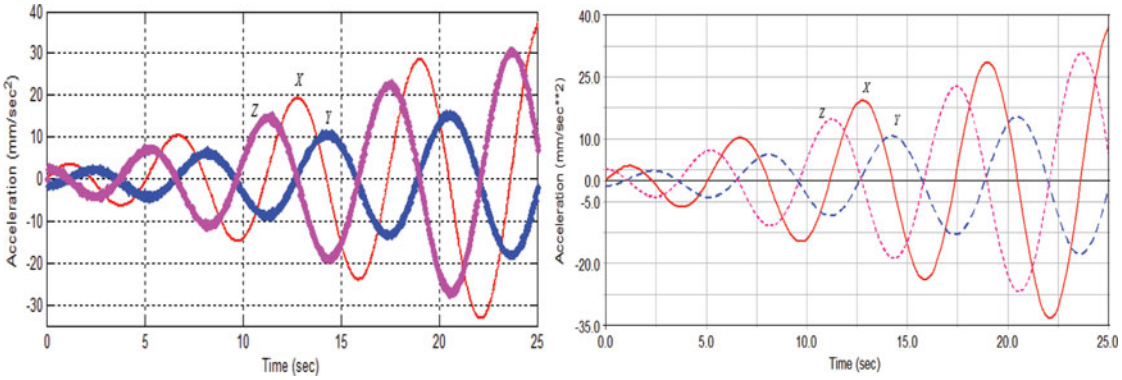


Fig. 8. Acceleration of point *P* for the entire path. Left: results of the proposed forward acceleration model; right: results using ADAMS©.

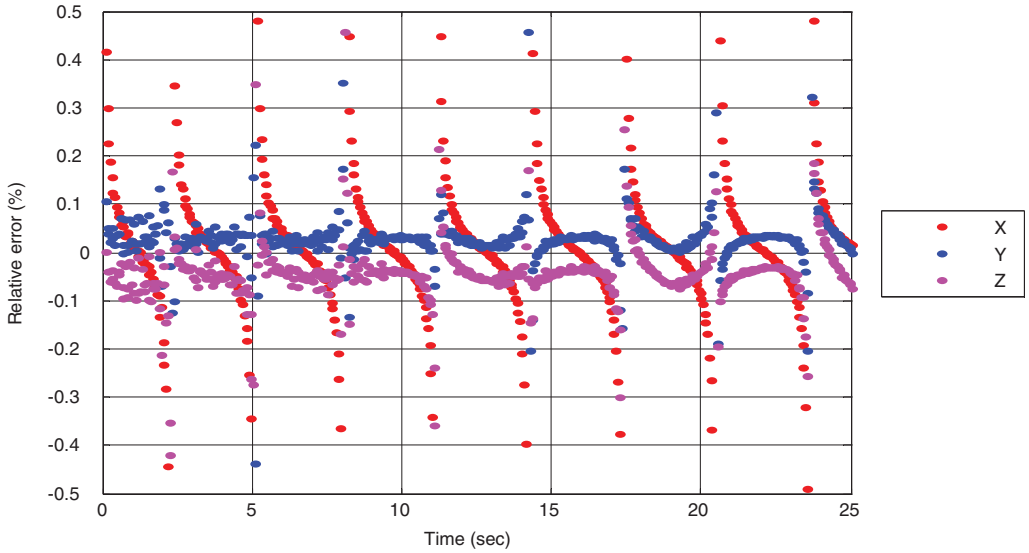


Fig. 9. Relative error of the acceleration model based on screw theory.

https://doi.org/10.1017/S0263574714002860 Published online by Cambridge University Press

the shape of the moving platform, greatly simplify the forward displacement model to find a semi-analytical form solution and reduce the presence of singularities.

The parallel robot introduced in this paper is an interesting proposal for a manipulator with industrial purposes. This mechanism maintains the traditional advantages of parallel manipulators over the serial one, e.g., load-carrying capacity, precise positioning and stiffness, but additionally offers advantages that are associated with the simplicity of a kinematic model and the reduction of singular configurations compared to other hexapods.

References

1. V. E Gough, "Contribution to Discussion to Papers on Research in Automobile Stability and Control and in Type Performance," *Proceedings of the Automation Division Institution of Mechanical Engineers*, UK (1957) pp. 392–365.
2. V. E. Gough and S. G. Whitehall, "Universal Tyre Testing Machine," *Proceedings of the FISITA Ninth International Technical Congress*, *IMechE 1*, London, UK (1962) pp. 117–137.
3. D. Stewart, "A Platform with Six Degrees of Freedom," *Proceedings of the Institution of Mechanical Engineers*, I (180), UK (1965) pp. 371–386.
4. R. Clavel, "Delta, a Fast Robot with Parallel Geometry," *Proceedings of the 18th International Symposium of Industrial Robots*, Lausanne (1988) pp. 91–100.
5. R. Clavel, "Device for the movement and positioning of an element in space," *US Patent No.* 4976582A, (Dec. 11, 1990).
6. K.-E. Neumann, "Robot," *US Patent No.* 4732525A, (Mar. 22, 1988).
7. B. Siciliano, "The Tricept robot: Inverse kinematics, manipulability analysis and closed-loop direct kinematics algorithm," *Robotica* **17**, 437–445 (1999).
8. F. Ronga and T. Vust, "Stewart Platforms without Computer?," *Proceedings of the Internnational Conference of Real, Analytic and Algebraic Geometry*, Trento (1992) pp. 197–212.
9. B. Mourrain, "The 40 Generic Positions of a Parallel Robot," *Proceedings of ISSAC'93*, Kiev (1993) pp. 173–182.
10. D. Lazard, "On the representation of rigid-body motions and its application to generalized platform manipulators," *J. Comput. Kinematics* **1**(1), 175–182 (1993).
11. M. Raghavan, "The Stewart platform of general geometry has 40 configurations," *ASME J. Mech. Des.* **115**(2), 277–282 (1993).
12. C. W. Wampler, "Forward displacement analysis of general six-in-parallel sps (Stewart) platform manipulators using soma coordinates," *Mech. Mach. Theory* **31**(3), 331–337 (1996).
13. M. Husty, "An algorithm for solving the direct kinematic of Stewart-Gough type platforms," *Mech. Mach. Theory* **31**(4), 365–379 (1996).
14. C. Innocenti, "Forward kinematics in polynomial form of the general Stewart platform," *ASME J. Mech. Des.* **123**(2), 254–260 (2001).
15. T.-Y. Lee and J.-K. Shim, "Forward kinematics of the general 6–6 Stewart platform using algebraic elimination," *Mech. Mach. Theory* **36**(9), 1073–1085 (2001).
16. T.-Y. Lee and J.-K. Shim, "Improved dialytic elimination algorithm for the forward kinematics of the general Stewart-Gough platform," *Mech. Mach. Theory* **38**(6), 563–577 (2003).
17. A.-X. Liu and T.-L. Yang, "Configuration Analysis of a Class of Parallel Structures using Improved Continuation," *9th World Congress on the Theory of Machines and Mechanisms*, Milan, Italy (1995) pp. 155–158.
18. Z. Mu and K. Kazerounian, "A real parameter continuation method for complete solution of forward position analysis of the general Stewart," *J. Mech. Des.* **124**(2), 236–44 (2002).
19. L. Rolland, "Certified solving of the forward kinematics problem with an exact algebraic method for the general parallel manipulator," *Adv. Robot.* **19**(9), 995–1025 (2005).
20. D. Gan, Q. Liao, J. S. Dai, S. Wei and L. D. Seneviratne, "Forward displacement analysis of the general 6–6 Stewart mechanism using Gröbner bases," *Mech. Mach. Theory* **44**(9), 1640–1647 (2009).
21. J.-P. Merlet, "Solving the forward kinematics of a Gough-type parallel manipulator with interval analysis," *Int. J. Robot. Res.* **23**(3), 221–235 (2004).
22. H. Shen and X. Wu, "Numerical solution of direct kinematic problems for parallel manipulators based on interval dividing search algorithms," *Mech. Sci. Technol.* **23**, 185–188 (2004).
23. S. Liu, W. Li, Y. Du and L. Fang, "Forward on Kinematics of the Stewart Platform using Hybrid Immune Genetic Algorithm," *Proceedings of the IEEE Conference on Mechatronics and Automation*, Luoyang (2006) pp. 2330–2335.
24. A. Omran, G. El-Bayiumi, M. Bayoumi and A. Kassem, "Genetic algorithm based optimal control for a 6-dof non redundant stewart manipulator," *In. J. Mech. Syst. Sci. Eng.* **2**(2), 73–79 (2008).
25. L. Rolland and R. Chandra, "On Solving the Forward Kinematics of the 6–6 General Parallel Manipulator with an Efficient Evolutionary Algorithm," *ROMANSY 18 Robot Design, Dynamics and Control: Proceedings of The Eighteenth CISM-IFToMM Symposium*, Springer Vienna, (2010) pp. 117–124.
26. P. J. Parikh and S. S. Lam, "A hybrid strategy to solve the forward kinematics problem in parallel manipulators," *IEEE Trans. Robot.* **21**(1), 18–25 (2005).

https://doi.org/10.1017/S0263574714002860 Published online by Cambridge University Press

27. S. N. Yurt, E. Anli and I. Ozkol, "Forward kinematics analysis of the 6–3 SPM by using neural networks," *Meccanica* **42**(2), 187–96 (2007).
28. J.-P. Merlet, "Closed Form Resolution of the Direct Kinematics of Parallel Manipulators Using Extra Sensors Data," *Proceedings of the 1993 IEEE International Conference on Robotics and Automation*, Atlanta (1993) pp. 200–204.
29. L. Baron and J. Angeles, "Kinematic decoupling of parallel manipulators using joint-sensor data," *IEEE Trans. Robot. Autom.* **16**(6), 644–651 (2000).
30. A. Zubizarreta, I. Cabanes, M. Marcos and Ch. Pinto, "Dynamic modeling of planar parallel robots considering passive joint sensor data," *Robotica* **28**(5), 649–661 (2010).
31. S.-L. Chen and I.-T. You, "Kinematic and singularity analyses of a six-DOF 6–3–3 parallel link machine tool," *Int. J. Adv. Manuf. Technol.* **16**(11), 835–842 (2000).
32. S.-L. Chen and Y.-C. Liu, "Post-processor development for a six degrees-of-freedom parallel-link machine tool," *Int. J. Adv. Manuf. Technol.* **18**(4), 254–265 (2001).
33. M. Zhang and B. Zhuo, "Workspace Analysis and Parameter Optimization of a Six-DOF 6–3–3 Parallel Link Machine Tool," *Intelligent Robotics and Applications, Lecture Notes in Computer Science*, 5928, (2009) pp. 706–712.
34. H. Gao, P. Xiao and H. Zhang, "Configuration Optimization of Physical Prototype for 6–3–3 Parallel Mechanism," *Proceedings of 2011 International Conference on Electrical and Control Engineering (ICECE)*, Yichang, China (2011) pp. 2937–2939.
35. J. Gallardo-Alvarado, M. García-Murillo and E. Castillo-Castaneda, "A 2(3-RRPS) parallel manipulator inspired by Gough-Stewart platform," *Robotica* **31**(3), 381–388 (2013).
36. M. García-Murillo, E. Castillo-Castaneda and J. Gallardo-Alvarado, "Dynamics of a 2(3-RRPS) Parallel Manipulator," *Proceedings of the 9th International Workshop on Robot Motion and Control*, Poland, (2013) pp. 270–275.
37. B. Mayer and C. Gosselin, "Singularity analysis and representation of the general Gough-Stewart platform," *Int. J. Robot. Res.* **19**(3), 271–288 (2000).
38. Z. Huang and Y. Cao, "Property identification of the singularity loci of a class of Gough–Stewart manipulators," *Int. J. Robot. Res.* **24**(8), 675–685 (2005).
39. S. Bandyopadhyay and A. Ghosal, "Geometric characterization and parametric representation of the singularity manifold of a 6–6 Stewart platform manipulator," *Mech. Mach. Theory* **41**(11), 1377–1400 (2006).
40. Q. Jiang and C. Gosselin, "Determination of the maximal singularity-free orientation workspace for the Gough–Stewart platform," *Mech. Mach. Theory* **44**(6), 1281–1293 (2009).
41. B. Dasgupta and T. S. Mruthyunjaya, "Singularity-free path planning for the Stewart platform manipulator," *Mech. Mach. Theory* **33**(6), 711–725 (1998).
42. S. Sen, B. Dasgupta and A. Mallik, "Variational approach for singularity-free path-planning of parallel manipulators," *Mech. Mach. Theory* **38**(11), 1165–1183 (2003).
43. O. Bohigas, M. Manubens and L. Ros, "Planning Singularity-Free Force-Feasible Paths on the Stewart Platform," *Latest Advances in Robot Kinematics*, Springer Netherlands, (2012) pp. 245–252.
44. F. Pierrot, M. Uchiyama, P. Dauchez and A. Fournier, "A new design of a 6-DOF parallel robot," *J. Robot. Mechatronics* **2**(4), 308–315 (1990).
45. J. Nielsen and B. Roth, "Formulation and Solution for the Direct and Inverse Kinematics Problems for Mechanisms and Mechatronic Systems," *Computational Methods in Mechanical Systems: Mechanism Aanalysis, Synthesis, and Optimization*, NATO ASI Series, Springer Berlin Heidelberg, vol. **161**, (1998) pp. 33–52.
46. J. Gallardo-Alvarado, C. Aguilar-Nájera, L. Casique-Rosas, L. Pérez González and J. Rico-Martinez, "Solving the kinematics and dynamics of a modular spatial hyper-redundant manipulator by means of screw theory," *Multibody Syst. Dyn.* **20**, 307–325 (2008).
47. J. M. Rico and J. Duffy, "An application of screw algebra to the acceleration analysis of serial chains," *Mech. Mach. Theory* **31**(5), 445–457 (1996).
48. J. M. Rico and J. Duffy, "Forward and inverse acceleration analyses of in-parallel manipulators," *ASME J. Mech. Des.* **122**(3), 299–303 (2000).
49. J. Gallardo-Alvarado, H. Orozco-Mendoza and R. Rodriguez-Castro, "Finding the jerk properties of multibody systems using helicoidal vector fields," *IMechE Part C, J. Mech. Eng. Sci.* **222**(11), 2217–2229 (2008).
50. T. Lung-Wen, *Robot Analysis: The Mechanics of Serial and Parallel Manipulators* (John Wiley & sons, INC., USA, 1999).
51. J. Gallardo-Alvarado, J. M Rico and G. Alici, "Kinematics and singularity analyses of a 4-dof parallel manipulator using screw theory," *Mech. Mach. Theory* **41**(9), 1048–1061 (2006).
52. C. Gosselin and J. Angeles, "Singularity analysis of closed-loop kinematic chains," *IEEE Trans. Robot. Autom.* **6**(3), 281–290 (1990).
53. I. Bonev, D. Zlatanov and C. Gosselin, "Singularity analysis of 3-DOF planar parallel mechanisms via screw theory," *J. Mech. Des.* **125**(3), 573–581 (2003).
54. E. Gross, S. Petrovic and J. Verschelde, "Interfacing with PHCpack," *J. Softw. Algebra Geom.* **5**, 20–25 (2013).

https://doi.org/10.1017/S0263574714002860 Published online by Cambridge University Press